

# APPLICATIONS OF TIME DOMAIN SIMULATION TO COUPLER DESIGN FOR PERIODIC STRUCTURES\*

N. M. Kroll<sup>1,2</sup>, C.-K. Ng<sup>1</sup> and D. C. Vier<sup>2</sup>

<sup>1</sup> Stanford Linear Accelerator Center, Stanford University, Stanford, CA 94309, USA

<sup>2</sup> University of California, San Diego, La Jolla, CA 92093, USA

## Abstract

We present numerical procedures for analyzing the properties of periodic structures and associated couplers based upon time domain simulation. Simple post processing procedures are given for determining Brillouin diagrams and complex field distributions of the traveling wave solutions, and the reflection coefficient of the traveling waves by the input and output. The availability of the reflection coefficient information facilitates a systematic and efficient procedure for matching the input and output. The method has been extensively applied to coupler design for a wide variety of structures and to a study directed towards elimination of the surface field enhancement commonly experienced in coupler cells.

## I. Introduction

Numerical simulation procedures for designing waveguide couplers to accelerator structures are described in [1] and an example of its application to the design of the input coupler for the NLC linac is given in [2]. A coupler cavity is designed with the intent of providing a matched connection between a waveguide and a uniform accelerator structure with dimensions corresponding to those of the cell adjacent to the coupler cavity. A symmetric structure consisting of two coupler cavities (with associated waveguides) connected by a short section of accelerator structure (typically two cells worth) is modeled and subjected to a (let us assume single frequency) time domain simulation. The entire assembly is treated as a single structure with two wave guide ports. The coupler cell dimensions are adjusted until an apparent match is achieved, that is, until no reflection is experienced at the ports (the external matching condition). To eliminate the possibility that the match arises from a fortuitous cancellation between forward and backward waves within the accelerator structure, both the amplitude and phase of the accelerating field on the beam axis are observed and required to have the periodicity and phase advance properties appropriate to a pure traveling wave (the internal matching condition). As a check one may add a cell to the accelerator structure and see whether all these conditions are still satisfied. It is often the case that accelerator structures are slowly varying rather than uniform, in which case the input and output couplers are matched separately.

In practice the procedure (we refer to it as the standard procedure) has been quite time consuming, involving trial

and error rather than a systematic procedure to simultaneously satisfy both the internal and external matching conditions. Another limitation arises from the fact that the method assumes that evanescent bands can be neglected but provides no procedure for demonstrating their absence.

In the next section we describe a new simulation procedure which has been found to be much more efficient, and also which provides information about the presence of evanescent bands. The basic elements of the method were briefly described in [3] in connection with the design of a coupler for the zipper structure. Because it has since replaced the old method for all of our coupler design work, a more complete presentation together with examples will be presented in the following sections.

## II. The New Simulation Procedure

As in the case of the old standard procedure one applies a single frequency time domain simulation by driving the input port of a two port structure consisting of an input cavity, an  $N$  cell periodic structure with period  $P$ , and an output cavity. Instead, however, of focusing attention on the  $S$  parameters of the structure as a whole, we direct our attention to the simulated accelerating field  $E_z(z, t)$  evaluated along the beam axis. We assume a steady state has been reached, so that the subsequent time dependence can be expressed in terms of the complex  $E_z(z)$  ( $E_c(z)$  henceforth), obtained in the standard way by combining the simulated real fields at two times separated by a quarter period. Then from Floquet's theorem (neglecting evanescent bands, losses, and an irrelevant overall phase factor)

$$E_c(z) = E(z)[\exp(-j\phi(z)) + R\exp(j\phi(z))]. \quad (1)$$

Here  $E(z)$  is a real positive amplitude function with period  $P$ , and  $\phi(z)$  is a real phase function, periodic except for a cell to cell phase advance  $\psi$ . Thus

$$E(z \pm P) = E(z), \text{ and } \phi(z \pm P) = \phi(z) \pm \psi. \quad (2)$$

$R$  is a  $z$  independent complex reflection coefficient. Note that one is free to shift  $\phi$  by an arbitrary constant with a compensating phase shift in  $R$ , since the overall phase of  $E_c$  is irrelevant. This freedom corresponds to the choice of reference plane through some point  $z_0$  where we take  $\phi = 0$ .

We now consider the quantities

$$\Sigma(z) = F^+(z) + F^-(z), \text{ and } \Delta(z) = F^+(z) - F^-(z), \quad (3)$$

where

$$F^\pm(z) = E_c(z \pm P)/E_c(z). \quad (4)$$

\*Work supported by the Department of Energy, contract DE-AC03-76SF00515, grants DE-FG03-93ER40759 and DE-FG03-93ER40793.

Elementary algebraic manipulation leads to the relations:

$$2\text{Cos}(\psi) = \Sigma(z), \quad (5)$$

$$\text{Re}xp(2j\phi) = [2\text{Sin}(\psi) - j\Delta(z)]/[2\text{Sin}(\psi) + j\Delta(z)]. \quad (6)$$

We note that while the RHS of (5) is formed of  $z$  dependent complex quantities, it nevertheless turns out to be real and  $z$  independent. Similarly the absolute value of the RHS of (6) is also  $z$  independent. Both these results should hold for all “allowed”  $z$  values, i.e., values such that the three points  $z+P$ ,  $z$ , and  $z-P$  all lie within the periodic portion of the structure simulated, and together they constitute a powerful constraint on the validity of the Floquet representation Eq. (1). Their failure beyond small numerical fluctuations or small deviation from steady state is evidence for the presence of evanescent bands. An example will be presented in the section on the Zipper structure.

It is noteworthy that these relations allow one to determine all the properties of the traveling wave solutions, including the functions  $\phi(z)$  and  $E(z)$  from a simulation which contains an arbitrary mixture of forward and backward waves. Of particular importance is the fact that it gives the magnitude and phase of the reflection coefficient. In contrast to the old standard method, there is here only one matching condition to be satisfied, namely  $|R| = 0$ . Typically match is achieved by varying two parameters in the coupler design. Once one has determined how the real and imaginary parts of  $R$  vary with the parameters, one can choose linear combinations of changes which accelerate the process of converging to the origin in the complex  $R$  plane [4]. Because the phase of  $R$  does depend upon the position of the reference point relative to the couplers, one naturally keeps it fixed while carrying out this process. Note that it is the output cavity that is matched by this procedure. While not necessary, it is usually convenient to construct a symmetric mesh. The input and output cavities are then the same, and the structure as a whole is matched when  $R$  vanishes.

### III. Applications and Examples

#### (a) The NLC four port output coupler

As an example of the principal features of the new method we use the new NLC four port output coupler cavity [5]. The purpose of the four port design was to provide damping for those dipole modes that reach the end of the structure while also providing an output for the accelerating mode. These dipole modes are typically those which had been poorly damped because of decoupling of the last cells from the manifolds. The four port symmetry provides damping for both dipole mode polarizations and has the added advantage of eliminating quadrupole distortion of the coupler fields.

The design simulation was carried out with a three cell periodic structure, and results are illustrated in Fig. (1). Two cases are shown, one matched, the other not. The reflection coefficients  $|R|$  as computed from Eq. (5) for the two cases are shown as functions of  $z$ . The allowed  $z$  values are those lying within the central cell, and one sees that for

both cases  $|R|$  is constant over that range. The real part of  $\text{Cos}(\psi)$  is also plotted as a function of  $z$ . One sees that the two values are indeed constant over the allowed range, but contrary to expectations they differ somewhat from each other and from the expected value of one half. This is due to the fact that a different and coarser mesh than that used to determine the phase advance parameter was used for the time domain simulations. The two cases differ from one another because the parameter variations in the coupler associated with the matching procedure induce small but global changes in the meshing. It has been confirmed in a number of cases that there is good agreement between the phase frequency relation determined from single cell periodic boundary condition frequency domain calculations and that determined from the time domain method described here so long as the same mesh is used for both simulations.

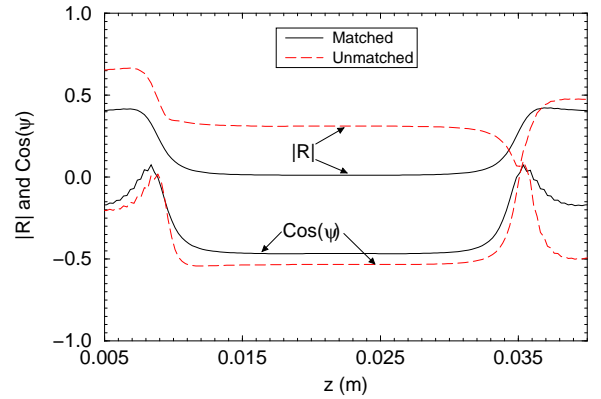


Figure 1  
 $|R|$  and  $\text{Cos}(\psi)$  along the axis of the NLC four-port output coupler.

#### (b) A Photonic Band Gap (PBG) structure

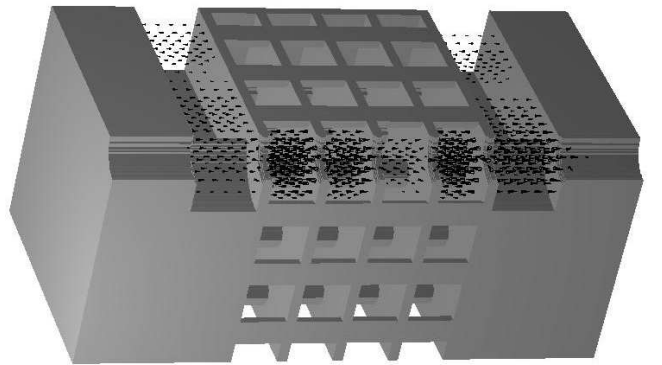


Figure 2  
A snapshot of electric field in the PBG structure.

A coupler cell very similar to those of the SLAC structures has been designed for a PBG structure, that is, a cylindrical cell with a pair of symmetrically placed waveguide ports, a conventional beam pipe, and conventional beam iris coupling to the periodic PBG structure. The PBG cell structure [6] is a seven by seven square array

of metallic posts aligned in the beam direction and terminated by metallic end plates, the cell cavity being formed by removing the central post. A circular aperture in the end plates, identical to that between the coupler cell and the adjacent PBG cell, provides cell to cell coupling and a path for the beam. A perspective representation of the four cell quarter structure used for the simulations is shown in Fig. (2). Also shown is the simulated electric field distribution, scaled logarithmically to enhance the visibility of weak field strengths. The figure illustrates the effectiveness of the PBG structure in confining the acceleration fields to the interior of the structure. The matching procedure worked well, and, as in the four port coupler above, there was no evidence for evanescent band contamination. Fabrication of an experimental model with 5 coupled PBG cells and complete with couplers is in progress at SLAC.

(c) *The Zipper structure*

The zipper is a planar accelerator structure described in [3]. A 25 (counting the coupler cavities) cell W band model has been built, cold tested, and subjected to bead pull measurements as reported in [7]. The design was governed by a decision to avoid bonded joints involving tiny structure elements such as the vanes which serve as cell boundaries and also form the beam iris. The coupler cell is a quarter wave transformer terminating in WR10 waveguide.

Early attempts at matching the coupler using the old standard method failed, and it was this failure which led to the development reported here. Matching using this method was accomplished by making use of a time domain simulation of a structure with 22 periodic cells. Fig. 3 shows the resultant  $Re Cos(\psi)$ ,  $Im Cos(\psi)$ , and  $|R|$  plots as computed from Eqs. (5) and (6). One sees large deviations from the expected  $z$  independent behavior as one moves away from the center of the structure. This effect indicates a clear violation of Eq. (1). From the fact that the violation fades away as one moves away from the couplers indicates that the effect is due to the couplers generating an evanescent band, the nearby monopole band pointed out in [3]. This example demonstrates how the method indicates the presence of evanescent band interference, and also how one can carry out the matching procedure even when it is present.

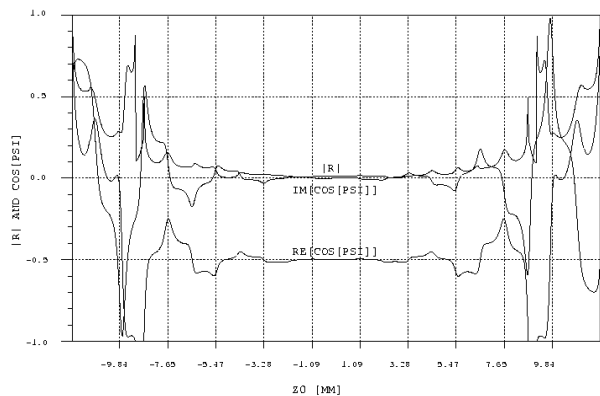


Figure 3

$|R|$  and  $Cos(\psi)$  along the axis of the zipper structure.

#### IV. The Coupler Field Enhancement Problem

Electrical discharge damage has been commonly observed in the coupler cells of accelerator structures and has been attributed to the field enhancement noted in simulations. We have taken advantage of our enhanced matching capability to initiate a study of this long standing problem. Exploration of the situation for the NLC coupler [2] showed that the largest enhancement occurred on the coupler side of the aperture of the iris separating the coupler from the adjacent cell with azimuthal maxima opposite the coupler waveguides and azimuthal minima 90 degrees away. This observation was consistent with the pattern of discharge damage [9]. It is pointed out in [8] that the azimuthal variation is due to the quadrupole component introduced by the coupler waveguides and that the enhancement can be reduced by introducing a racetrack like modification of the coupler cell shape designed to eliminate it. This effect and its cure have been confirmed in our own studies of the NLC coupler. Two other modifications have also been explored. The simplest and most effective was simply to reduce the radius of the cell adjacent to the coupler. The effect for a 2% reduction is illustrated in Fig. 4 where it is seen that the field on the coupler cell iris is significantly less than that on the interior coupling irises. An undesirable consequence is a 10 degree phase advance deficiency in the modified cell. An even larger field reduction would be obtained by removing the quadrupole enhancement. We attribute the reduction to an increase in group velocity. The other modification consisted of enlarging the coupler iris combined with an increase in the adjacent cell radius chosen so as to preserve the cell phase advance, but the exploration of this effect is incomplete. Experimental investigation to determine whether such changes actually do reduce electrical discharge damage in the coupler is clearly needed.

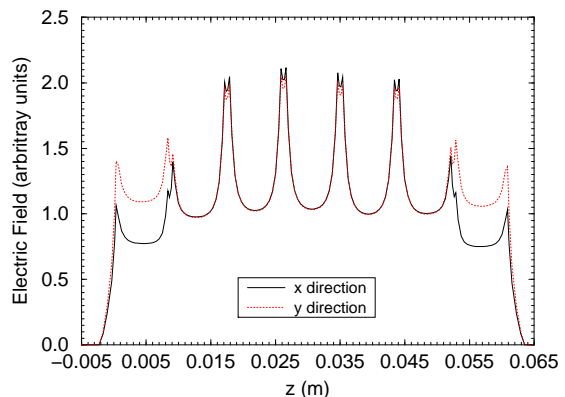


Figure 4

$z$  variation of electric field magnitude at radial positions of the beam irises.

#### References

- [1] C.K. Ng and K. Ko, Proc. CAP93 p243 1993
- [2] G.B. Bowden et al, Proc. PAC99 p3426 1999
- [3] N.M. Kröll et al Proc. PAC99 p3612 1999
- [4] We are indebted to Roger H. Miller for suggesting this procedure and emphasizing the advantage of tracking the complex  $R$  rather than  $|R|$ .

- [5] J.W. Wang, et al, Oral Poster TUA3, This Conference; R.M. Jones, et al, Poster TUA8, This Conference
- [6] D.R. Smith, et al, AAC94, AIP Conf. Proc. 335, p761 (1995)
- [7] D.T. Palmer, et al, The Design, Fabrication, and RF Measurements of the First 25 cell W-Band Constant Impedance Accelerating Structure, AAC2000, to appear in AIP Conf. Proc. for AAC2000
- [8] J. Haimson, B. Mecklenberg, and E.L. Wright, AAC96, AIP Conf. Proc. 398, p898 (1997)
- [9] Juwen Wang, private communication